

Mechanistic Studies of Pd-Catalyzed Fluorination of Cyclic Vinyl Triflates: Evidence for *in situ* Ligand Modification

Yuxuan Ye,^{†,||} Seoung-Tae Kim,^{‡,§,||} Ryan P. King,[†] Mu-Hyun Baik,^{§,‡,*} Stephen L. Buchwald^{†,*}

[†]Department of Chemistry, Massachusetts Institute of Technology, Cambridge, MA 02139, USA

[‡]Department of Chemistry, Korea Advanced Institute of Science and Technology (KAIST), Daejeon, 34141, Republic of Korea

[§]Center for Catalytic Hydrocarbon Functionalizations, Institute for Basic Science (IBS), Daejeon, 34141, Republic of Korea

Pd-catalyzed nucleophilic fluorination reactions are important methods for the synthesis of fluoroarenes and fluoroalkenes. However, these reactions can generate a mixture of regioisomeric products that are often difficult to separate. While investigating the Pd-catalyzed fluorination of cyclic vinyl triflates, we observed that the addition of a substoichiometric quantity of TESCOF₃ significantly improves both the efficiency and the regioselectivity of the fluorination process. Herein, we report a combined experimental and computational study on the mechanism of this transformation focused on the role of TESCOF₃. We found that in the absence of additives such as TESCOF₃, the transmetalation step produces predominantly the thermodynamically more stable *trans* isomer of the key LPd(vinyl)F complex (L = biaryl monophosphine ligand). This intermediate, rather than undergoing reductive elimination, preferentially reacts through an intramolecular β-deprotonation to form a Pd-cyclohexyne intermediate. This undesired reactivity is responsible for the low efficiency (11% yield) and poor regioselectivity (1.8:1) of the catalytic reaction. When TESCOF₃ is added to the reaction mixture, the *cis*-LPd(vinyl)F complex is instead formed, through a pathway involving an unusual dearomatization of the ligand by nucleophilic attack from a trifluoromethyl anion (CF₃[−]). In contrast to the *trans* isomer, this *cis*-LPd(vinyl)F complex readily undergoes reductive elimination to provide the vinyl fluoride product with desired regioselectivity, without the generation of Pd-cyclohexyne intermediates.

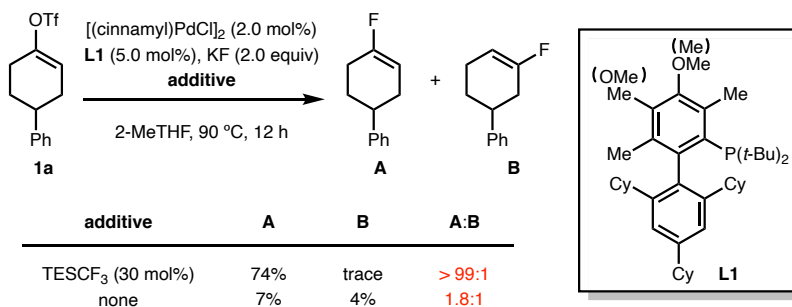
Introduction

Fluorine-containing molecules¹ are a valuable class of compounds with wide applications^{2,3} and desirable biological properties.⁴ Pd^{0/II}-catalyzed C–F cross-coupling is an attractive approach for the preparation of fluorinated compounds from readily available starting materials.^{5,6} Due to the challenging C–F reductive elimination from a Pd(II) intermediate,⁷ this transformation was not realized until recently.⁸

The generation of undesired regioisomeric fluorinated side products is a significant obstacle affecting Pd^{0/II}-catalyzed fluorination reactions.^{8b,9c} Previous mechanistic studies on the fluorination of aryl triflates indicated that the Pd-benzyne intermediates, generated from a base-induced elimination pathway, are responsible for producing undesired regioisomers.^{9c} In certain cases, nonpolar solvents such as cyclohexane could be used instead of polar solvents to minimize this undesired process.^{8a,8d} In addition, catalysts based on new ligands were developed, which promoted the aromatic fluorination reaction with higher degrees of regioselectivity and reactivity.^{8d,8e}

In 2016, motivated by the utility of fluorine-substituted olefins as amide surrogates in medicinal chemistry and chemical biology,^{10,11} we developed a Pd^{0/II}-catalyzed fluorination of cyclic vinyl triflates.¹² The addition of TESCF₃ to the reaction mixture was found to significantly improve both the yield and regioselectivity of the fluorination process. Under the standard reaction conditions using 30 mol% TESCF₃ as the additive, the desired fluorinated product **A** was generated in high yield with excellent regioselectivity (Scheme 1, with TESCF₃, 74% yield, **A**:**B** > 99:1). However, in the absence of TESCF₃, the same reaction provided the fluorinated products in low yield and poor regioselectivity (Scheme 1, without TESCF₃, 11% combined yield, **A**:**B** = 1.8:1).

Scheme 1. Pd-Catalyzed Fluorination of Cyclic Vinyl Triflates.



A better understanding of the “TESCF₃ effect” in this fluorination process could provide insight into the mechanism of the fluorination reactions in general and also potentially allow us to expand this strategy to other Pd-catalyzed fluorination systems. Therefore, we undertook a

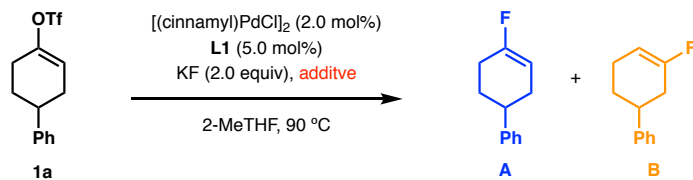
combined experimental and computational study on the fluorination of cyclic vinyl triflates, comparing the mechanisms of reaction with and without TESCF₃ as an additive. During our study, we uncovered a hitherto unrecognized transmetalation mechanism with fluoride involving an unusual dearomatization of the ligand by nucleophilic attack by a CF₃[−] nucleophile.

Results and Discussion

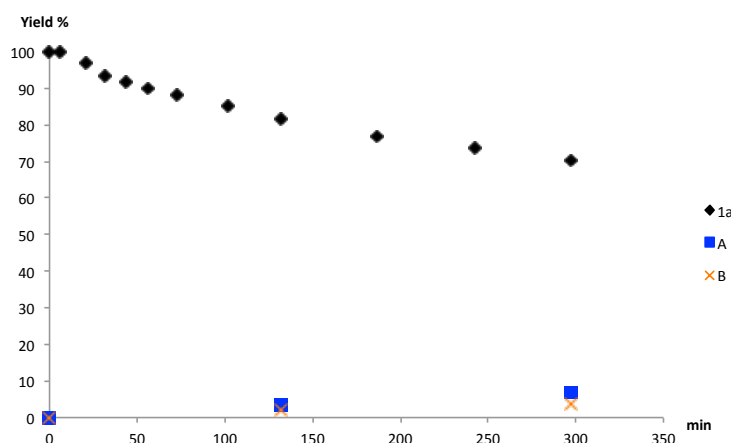
Kinetic Profiles of the Fluorination Reaction with and without TESCF₃ Additive

We commenced our investigation by monitoring the progress of a model reaction with and without TESCF₃ using ¹⁹F NMR analysis. In the absence of TESCF₃, after 5 h, a mixture of isomeric products was formed in *ca.* 10% combined yield with poor selectivity (Figure 1, without TESCF₃). In a separate reaction in which 30 mol% TESCF₃ was used as an additive, in the initial stage of the reaction (*t* = 0–120 min), no vinyl fluoride products were formed. During this time, TESCF₃ was continually consumed, and approximately 15% of **1a** decomposed via an unknown pathway. Then, after the TESCF₃ was fully consumed, the fluorination proceeded smoothly providing the desired vinyl fluoride product **A** in good yield (70% yield in 4 h) and with excellent regioselectivity (Figure 1, with TESCF₃). Compared to the kinetic profile without TESCF₃, the addition of a substoichiometric amount of TESCF₃ had a dramatic impact on the reaction in several ways. First, the rate of the fluorination process was increased and the regioselectivity was significantly improved. We hypothesized that a new catalytic species with better fluorinating activity might be forming in the presence of TESCF₃. Second, an induction period was observed at the beginning of the reaction, during which time no fluorinated product was formed. We reasoned that the presence of TESCF₃ inhibited the fluorination process, because fluoride anions would react preferentially with TESCF₃, preventing the generation of any Pd–F species that is required for product formation.¹³ It was probable that of the 30 mol% TESCF₃ added at the beginning of the reaction, only a small amount participated in the formation of the active catalyst species, while the rest decomposed to either CHCF₃ or CF₂CF₂ (observed by ¹⁹F NMR analysis of the crude reaction mixture) under the reaction conditions. We found that approximately 30 mol% was the minimal amount of TESCF₃ required to achieve the optimal regiochemical ratio of products (see the Supporting Information for details).

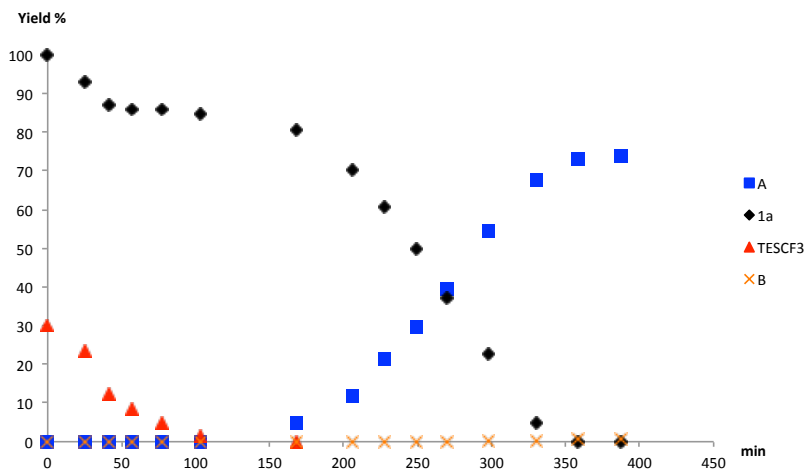
Figure 1. Reaction Kinetic Profiles with and without TESCF₃ as an Additive.^a



without TESCF₃:



with 30% TESCF₃:



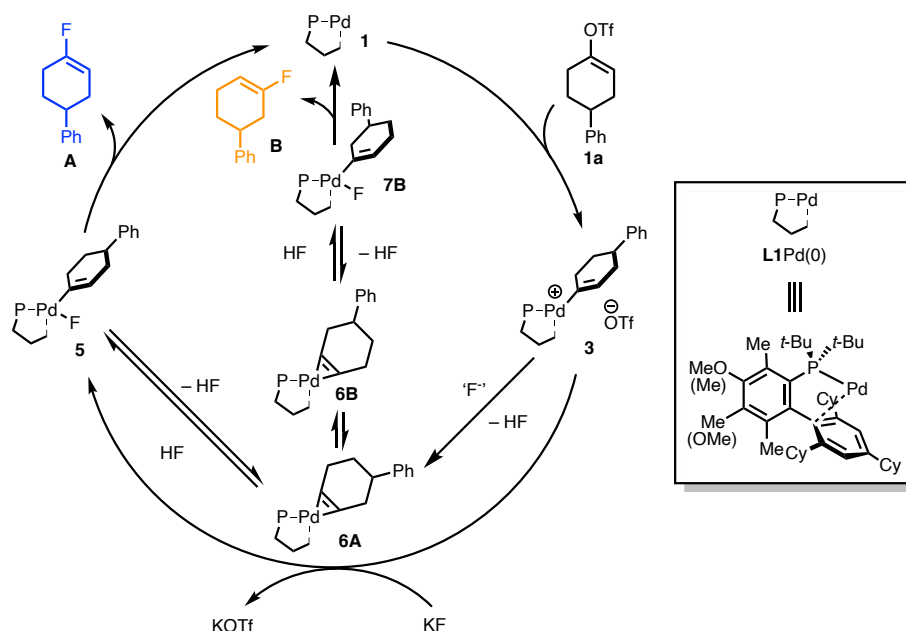
^aThe reaction was conducted at 1.0 mmol scale. Yields were determined by ¹⁹F NMR analysis of aliquots taken from the reaction mixture using 1-fluoronaphthalene as an internal standard.

Proposed mechanism of the fluorination reaction without TESCF₃

Based on our previous studies on Pd-catalyzed aromatic fluorination,^{8b} we proposed that the catalytic mechanism without any additives is as illustrated in Scheme 2. The productive fluorination process would initiate through the oxidative addition of vinyl triflate **1a** at the phosphine-ligated Pd(0) species **1** to form L1Pd(vinyl)(OTf) (**3**). Transmetalation with KF would

generate **L1Pd(vinyl)F (5)**, and C–F reductive elimination from **5** would provide the fluorinated product **A**. Alternatively, the Pd(II)-vinyl species, such as **3** and **5**, could undergo intramolecular deprotonation at the vinylic position to form an **L1Pd(II)-cyclohexyne intermediate 6A**, eliminating HF in the process. If possible, rapid, reversible isomerization of **6A** into **6B** would explain the formation of the regioisomeric vinyl fluoride product **B**. Specifically, the reaction of **6B** with HF would provide **L1Pd(vinyl')F (7B)**, which could undergo C–F reductive elimination to generate the vinyl fluoride **B** with the undesired regioselectivity.

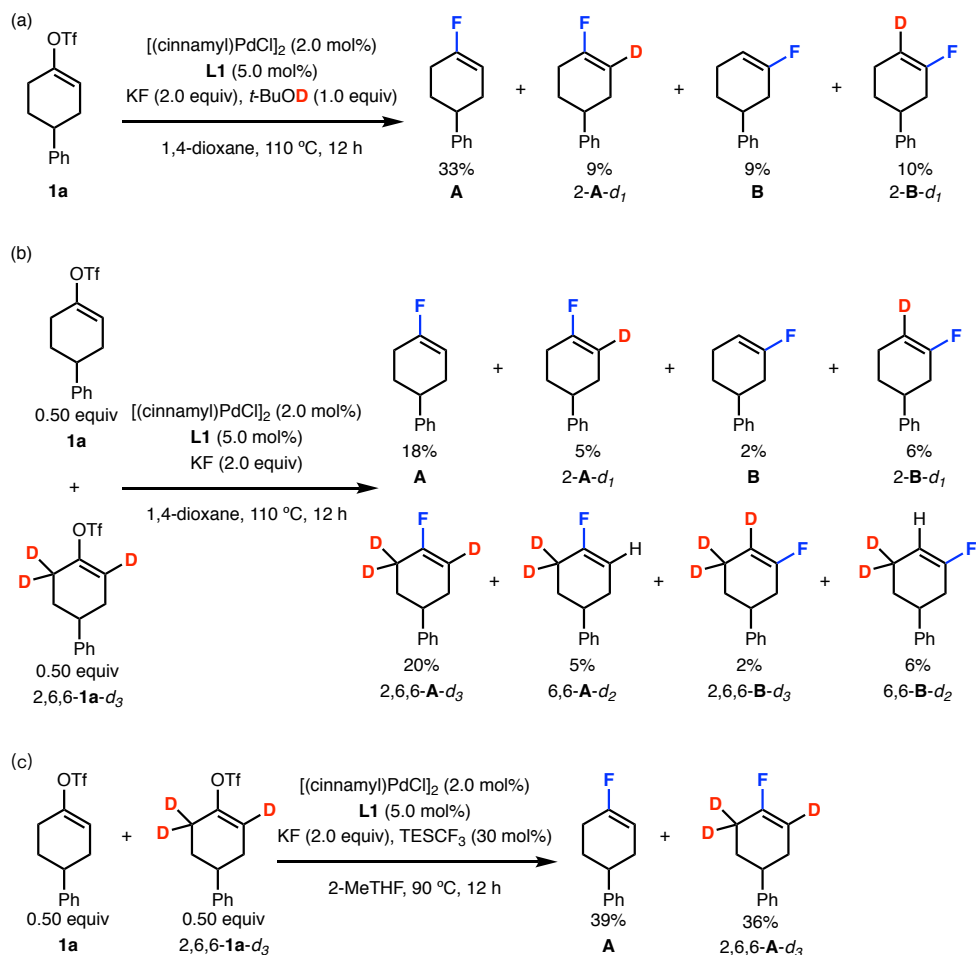
Scheme 2. Proposed Catalytic Cycle for Pd(II)-Catalyzed Fluorination of Cyclic Vinyl Triflates in the Absence of TESCF₃.



The reversible generation of **6A** and **6B** would be associated with the liberation of HF, and therefore, we could evaluate the plausibility of this pathway by carrying out the reaction in the presence of an exchangeable deuterium source.^{9c} Under these conditions, the reaction would presumably form DF *in situ*, which could recombine with **6A** and **6B** to incorporate deuterium into the appropriate positions of the vinyl fluoride products. When 1.0 equiv of *t*-BuOD was added to the reaction mixture, in addition to the formation of products **A** and **B**, significant amounts of deuterated products **2-A-d₁** and **2-B-d₁** were also observed by ¹⁹F NMR and confirmed by GC/MS (Scheme 3a). Additionally, a crossover experiment using **1a** and 2,6,6-A-d₃ provided eight products, representing the isotopologues of **A** and those of its regioisomer **B** (Scheme 3b). The observed protium–deuterium exchange at the 2-position is consistent with the involvement of the **L1Pd(II)-cyclohexyne intermediates (6A and 6B)**.

We wanted to test whether the improvements in regioselectivity associated with the addition of TESCF₃ might be due to an avoidance of these cyclohexyne intermediates. Thus, we conducted an analogous deuterium-labeling crossover experiment in the presence of 30 mol% TESCF₃ (Scheme 3c). In this experiment, **A** and 2,6,6-**A**-d₃ were the only fluorination products formed, and no deuterium crossover or regioisomeric products were observed. Thus, the pathways involving L1Pd(II)-cyclohexyne intermediates (**6A** or **6B**) were indeed not operative under these conditions.

Scheme 3. Deuterium Labeling Experiments Under TESCF₃-Free Conditions.^a



^aReactions were run at 0.10 mmol scale and at elevated temperature (110 °C) and 1,4-dioxane to get better yields for analysis. Yields were determined by ¹⁹F NMR analysis of the crude reaction mixture using 1-fluoronaphthalene as an internal standard. In (c), maximum yield is 50% for each of **A** and **A**-d₃.

DFT Calculations on the Mechanism of the Fluorination Reaction without TSCF₃

To gain further insight into these experimental observations, we evaluated the proposed mechanism with the aid of density functional theory (DFT) calculations. Geometry optimization, vibration, and solvation energy calculations were performed with M06/LACVP/6-31G** level of theory, and the electronic energies of all optimized structures were reevaluated with M06/LACV3P/cc-pVTZ(-f).¹⁴ Greater details of the computational methods are given in the supporting information. As shown in Figure 2, L1Pd(0) (**1**) engages **1a** through an initial π -complex **2**, from which oxidative addition proceeds with a barrier of 12.7 kcal/mol (via transition state **2-TS**) to afford L1Pd(vinyl)OTf (**3**). Subsequent dissociation of the triflate counterion from **3** gives the intermediate L1Pd(vinyl)⁺ (**4**). The ensuing addition of a fluoride anion to intermediate **4** could potentially provide either the *trans*-isomer **5** or the *cis*-isomer **5A**, in which the name indicates whether fluoride is bound *trans* or *cis* to the phosphine ligand, respectively. DFT calculations showed that the *trans*-isomer **5** is 2.4 kcal/mol lower in energy than **5A** due to the relative *trans* influences of the ligand on palladium. In addition, the dissociation energy of fluoride from **5** is 10.1 kcal/mol lower than from **5A**, indicating **5** would be formed dominantly in the reaction. This is consistent with what we observed previously in the aromatic fluorination reactions.^{8a}

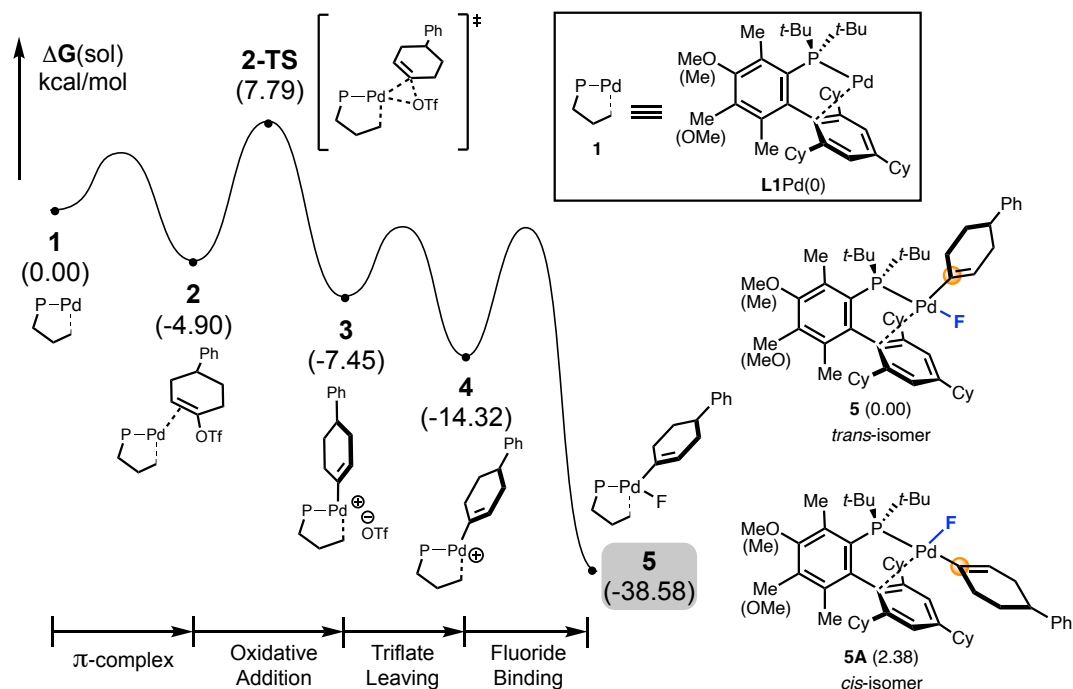


Figure 2. Energy profiles of partial of the proposed mechanism under TSCF₃-free conditions with optimized structure of **5** and **5A**.

As the *trans*-isomer **5** is the major isomer generated after fluoride association, we considered the reactivity of this complex. As shown in the proposed mechanism (Scheme 2), **5** could either provide the fluorinated product **A** via reductive elimination or undergo deprotonation to yield the **L1Pd(II)**-cyclohexyne intermediate **6A**. DFT calculations indicated that the reductive elimination from **5** is associated with a barrier of 24.9 kcal/mol via **5-TS**, while the competing deprotonation to form **6A** requires a lower activation energy of 22.2 kcal/mol via **6A-TS** (Figure 3). The 2.7 kcal/mol energy difference favoring deprotonation suggested that the generation of the **L1Pd(II)**-cyclohexyne intermediate **6A** is significantly favored over the productive reductive elimination pathway. Once **6A** is formed, it readily rearranges to **6B** through rotation of the cyclohexyne group (via **6AB-TS**), with an approximate barrier of 10 kcal/mol. Recombination of **6B** and HF generates **7B** (the *trans*-isomer is preferentially formed due to *trans* influence, see the Supporting Information for details). As with **5**, **7B** also favors deprotonation, regenerating **6B**, rather than reductive elimination. The calculations suggest that a Curtin–Hammett situation is operative in the vinyl fluorination process when additive is absent: **5** and **7B** rapidly interconvert via **L1Pd(II)**-cyclohexyne intermediates, each proceeding slowly but irreversibly to a different isomer of product (**A** and **B**, respectively) with low selectivity.

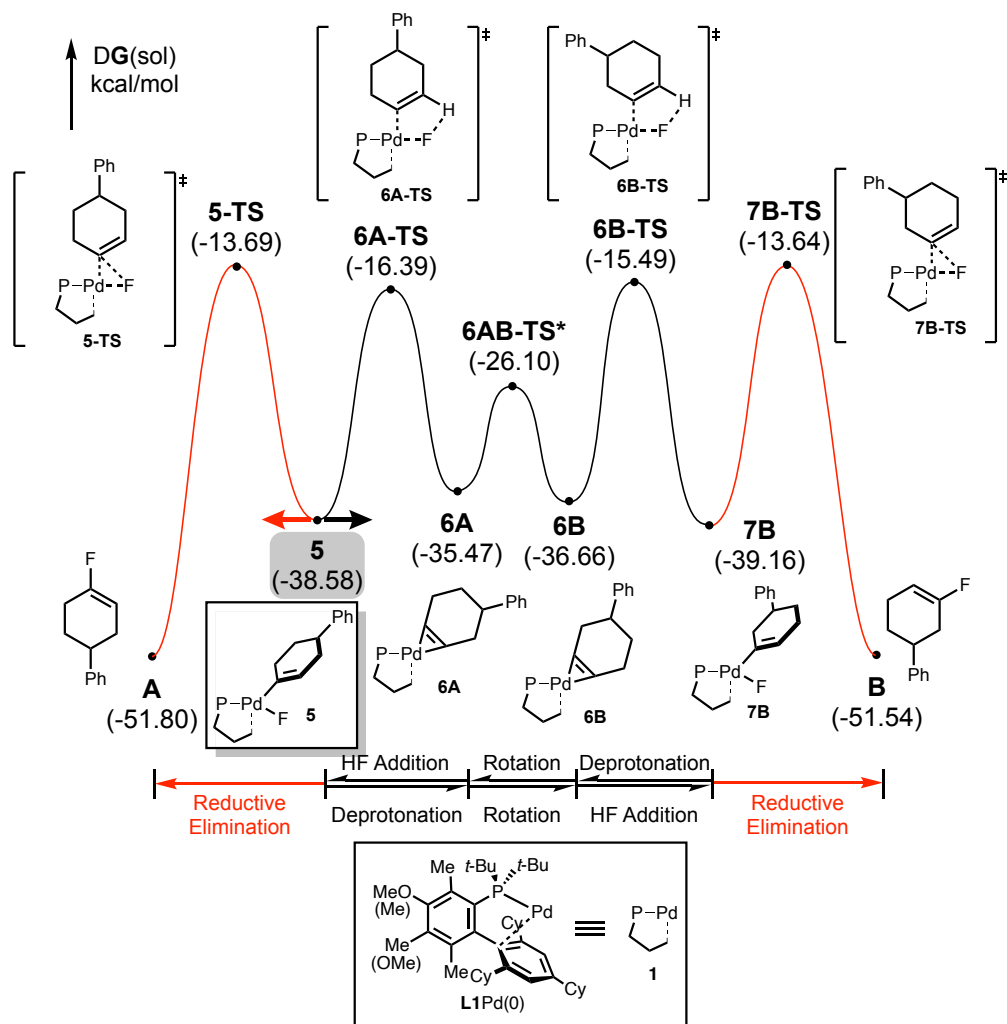
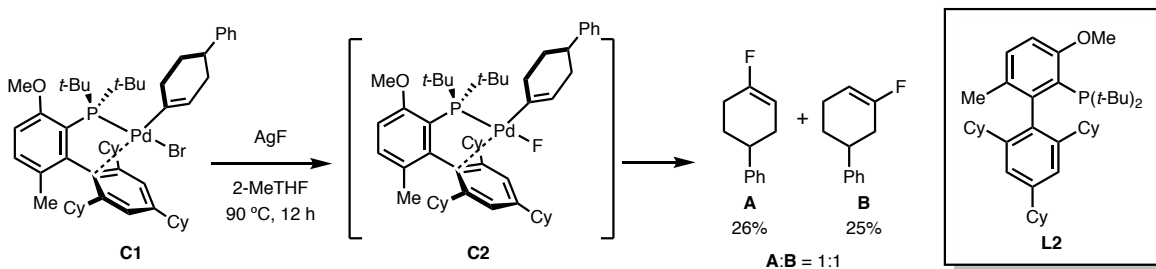


Figure 3. Energy profile of potential transformations of **5**.

We tried to prepare the *trans*-LPd(vinyl)F (**5**) intermediate and experimentally study its stoichiometric reactivity. As the preparation of Pd(II) complexes supported by **L1** is difficult, presumably due to the large size of **L1**, we employed **L2** as the supporting ligand for these stoichiometric studies (Scheme 4). As previously reported, **L2** was also effective in vinyl fluorination, although the regioselectivity of the process was slightly lower than that using **L1**.¹² We initially sought to prepare *trans*-L2Pd(vinyl)F (**C2**) from *trans*-L2Pd(vinyl)Br (**C1**) via salt metathesis with AgF. When **C1** was treated with AgF, fluorinated products **A** and **B** were readily formed, even at room temperature. This relatively rapid formation of product demonstrates the ability of bulky biarylphosphine ligands to facilitate C–F reductive elimination from Pd(II) complexes at ambient temperature. When the metathesis reaction was attempted in 2-MeTHF at 90 °C, which is the combination of solvent and temperature used in the catalytic reaction, **A** and **B** were generated in 26% and 25% yields, respectively, as assessed by ¹⁹F NMR. This observation is

consistent with the estimated theoretical regioselectivity (1:1) based on the computed energies using **L2** (see the Supporting Information for details).

Scheme 4. Stoichiometric Study on the Reductive Elimination of **C2**.



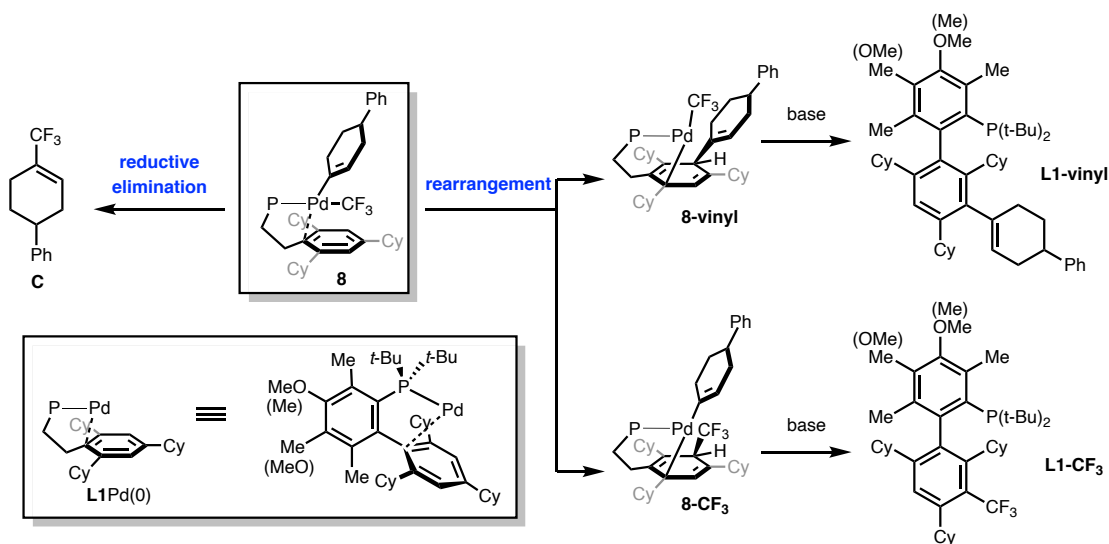
One Potential Role of TESCF_3 Additive: Formation of LPd-CF_3 Species

With an understanding of the fluorination process absent any additives, we then considered the potential role of TESCF_3 additive in the fluorination reaction. We envisioned that the CF_3^- released from TESCF_3 under the fluorination conditions might attack L1Pd(vinyl)^+ (**4**) to generate the L1Pd(vinyl)CF_3 complex, as was proposed in Pd-catalyzed trifluoromethylation reactions (Scheme 5, **8**).^{15–18} In a potential unproductive pathway, **8** could undergo reductive elimination to provide the trifluoromethylated side product **C** (Scheme 5, reductive elimination). However, even in the presence of 1.0 equiv of TESCF_3 , only trace amounts of side product **C** were observed in the fluorination reaction. Alternatively, **8** might serve as a precursor for an *in situ* modified ligand with improved catalytic activity and selectivity. Previously, in Pd-catalyzed aromatic fluorination reactions, we observed that the oxidative addition complex $t\text{-BuBrettPhosPd}(4\text{-}n\text{-Bu-C}_6\text{H}_4)\text{Br}$ (**D1**) underwent a dearomative rearrangement to generate **D2**, which upon deprotonation formed ligand-modified species **L3Pd** (Scheme 6).^{9a} This complex, based on modified ligand **L3**, is believed to be the active catalyst throughout most of the palladium-catalyzed aryl fluorination process. We hypothesized that **8** could undergo a similar dearomative rearrangement to generate ligands that are modified by the addition of an alkenyl or trifluoromethyl group (Scheme 5, rearrangement). We therefore sought to independently prepare these modified ligands and evaluate the reactivity and selectivity of reactions using catalysts based on them. For ease of synthesis, ligand **L4**, which is structurally similar to **L1** and which was also associated with a significant TESCF_3 effect in the fluorination reactions, was employed in the fluorination reaction and compared against its trifluoromethylated and alkenylated analogs (Table 1, entry 1 and 2).¹⁹ The use of neither of these modified ligands showed results comparable to the use of **L4** as the ligand with TESCF_3 as the additive. When the cyclohexenyl-modified version of **L4** (**L4-vinyl**) was used under TESCF_3 -free conditions, the reaction afforded the fluorinated products in 14% combined yield with 1.8:1

regioselectivity (Table 1, entry 3). The use of CF₃-modified ligand **L4-CF₃** under the same reaction conditions gave trace amount of the fluorination products (Table 1, entry 4). Moreover, when TESCF₃ was added to reactions using either **L4-vinyl** or **L4-CF₃** as the ligands, although less significant than the standard reaction condition using **L1**, improvements in regioselectivity and reactivity were observed (Table 1, entry 5 and 6). Together, these experiments suggest that an *in situ* 3'-substitution of the phosphine ligand did not account for the observed TESCF₃ effect.

Accordingly, we had to consider that the Pd-CF₃ intermediate **8** may not be formed at all in this fluorination process. The rigidity of the ligand backbone and the steric hindrance of the two *tert*-butyl groups on the phosphorous of these ligands (**L1** and **L2**) might render CF₃⁻ attack on the cationic Pd(II) center rather slow.^{20a,b} Consistent with this observation, palladium catalysts bearing *Pt*-Bu₂ ligands have been observed to be incompetent for Pd^{0/II}-catalyzed aryl trifluoromethylation, despite the associated C-CF₃ reductive elimination barrier being thermally accessible.^{20c}

Scheme 5. Proposed Formation of L1Pd(vinyl)CF₃ (8**) and Its Potential Impact on Fluorination Process.**



Scheme 6. Dearomative Rearrangement of the Oxidative Addition Complex in the Fluorination of Aryl Bromides.

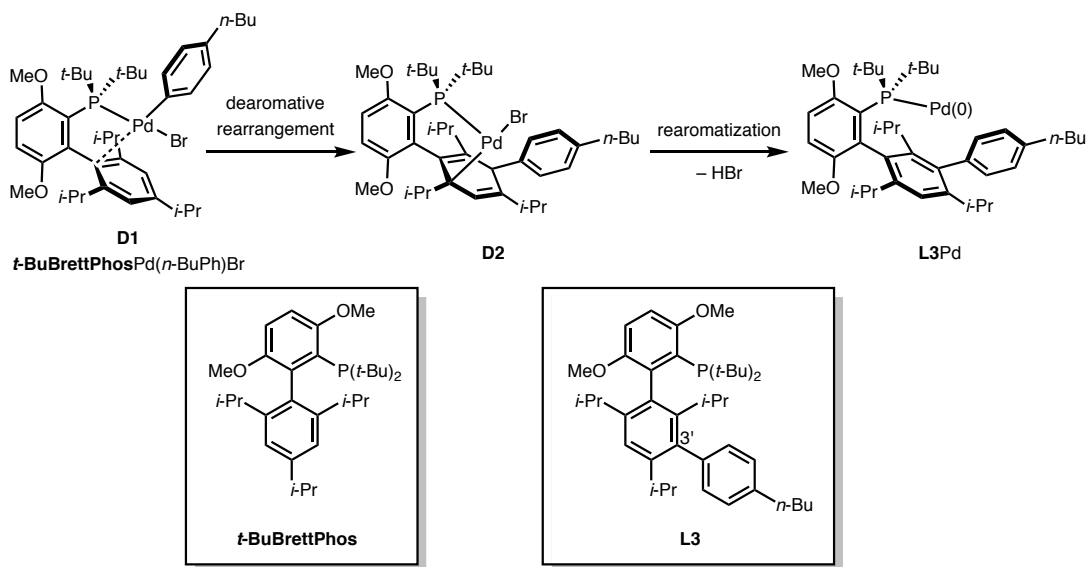
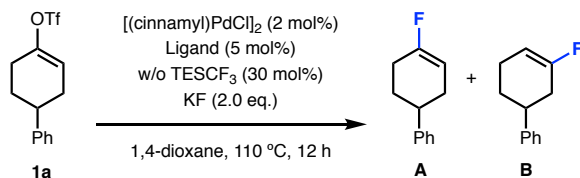
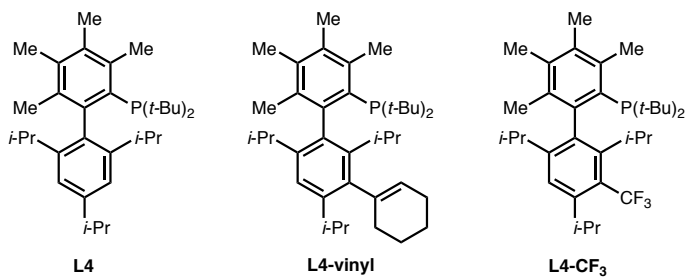


Table 1. Fluorination Reaction Employing Ligand L4, L4-vinyl and L4-CF₃.



entry	ligand and TESCOF ₃	A (%)	B (%)	A:B
1	L4	11	8	1.4:1
2	L4 + TESCOF₃	56	6	9.3:1
3	L4-vinyl	9	5	1.8:1
4	L4-CF₃	trace	trace	/
5	L4-vinyl + TESCOF₃	67	3	22:1
6	L4-CF₃ + TESCOF₃	21	2	11:1

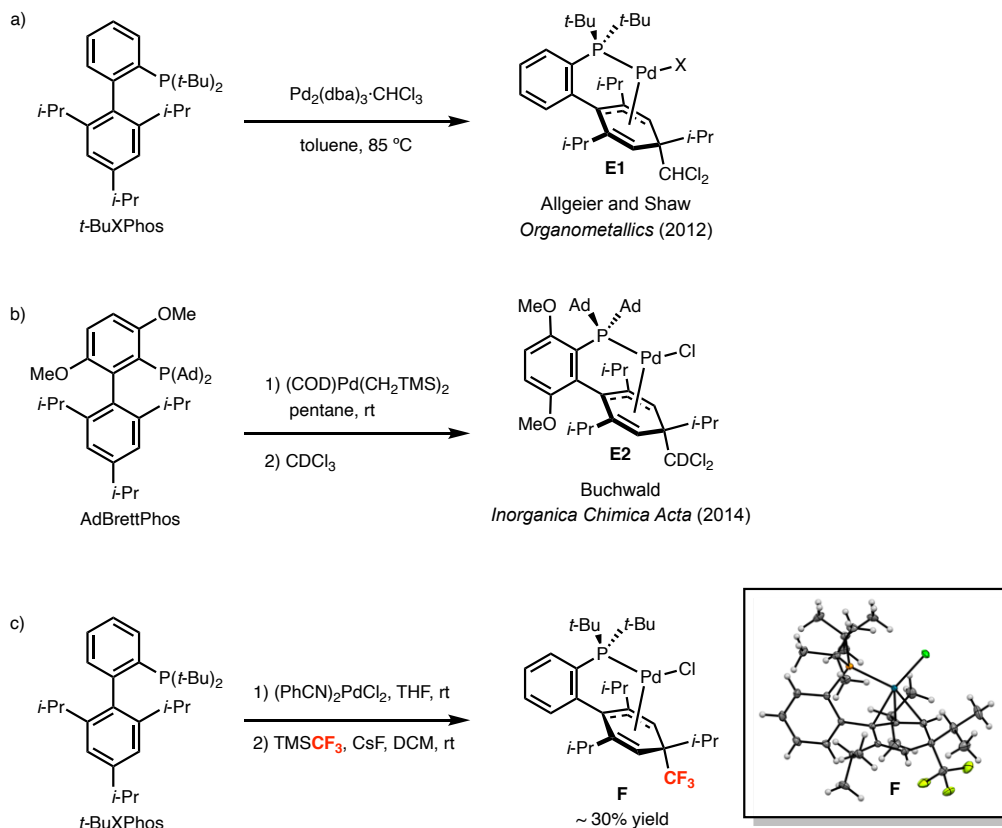


^aReactions were run at 0.10 mmol scale. Yields were determined by ¹⁹F NMR analysis of the crude reaction mixture using 1-fluoronaphthalene as an internal standard.

An Alternative Role of TESCF₃: Ligand Dearomatization

In searching for other potential roles for TESCF₃, our attention was drawn to a 2012 report from Amgen chemists in which they observed the generation of complex **E1** (Scheme 7a, **E1**) with a dearomatized ligand during Pd-catalyzed cross-coupling.^{21a} It was proposed that the dichlorocarbene, which formed from chloroform under basic conditions, attacked the bottom ring of *t*-BuXPhos and formed a bond at the *para*-position, on the face *anti* to the palladium. In 2014, our group also observed a similar dearomatized complex when exposing AdBrettPhos-Pd(0) to CDCl₃ (Scheme 7b, **E2**).^{21b,c} We wondered if such an analogous process could occur in the fluorination reaction wherein the trifluoromethyl anion (CF₃⁻) or the difluorocarbene (:CF₂) attacks the *para*-position of the bottom ring of the ligand. We found experimentally that in the presence of TMSCF₃ and a fluoride source, a dearomatized Pd(II) complex supported by *t*-BuXPhos was generated in approximately 30% yield in two steps (Scheme 7c, **F**). Single-crystal X-ray diffraction structure analysis demonstrated that **F** was structurally similar to **E1** and **E2**. In this case, the structure possesses an α -disposed CF₃ substituent at C4 position of a dearomatized ring, while the Pd center binds to the dienyl system in an η^3 fashion.

Scheme 7. Discovery of Pd Complexes Supported by Dearomatized Ligand.



Using **L1** as the supporting ligand, however, we were not able to prepare any of the Pd(II) complexes stoichiometrically, presumably due to the extreme steric properties of the ligand. Thus, in order to investigate the plausibility of this dearomative process for **L1** and its potential consequences on the fluorination process, DFT calculations were performed (Figure 4). Starting from **4'**, we found that the addition of CF_3^- to the bottom ring of the ligand demands an activation energy of 10.5 kcal/mol via transition state **4'-TS*** to form a dearomatized intermediate **6**.^{20b,22} The barrier indicates the dearomatization process is possible for **L1** under the fluorination reaction conditions. Further, because **4'** is a cationic complex, this dearomative process releases a substantial amount of energy (29.1 kcal/mol).

After the generation of **6**, reaction with a fluoride anion would form intermediate **7** or **7'**, where the fluoride is bound either in *cis* or *trans*-position to the phosphine ligand. Unlike in the case of **5** and **5A** where the *trans*-isomer **5** is more stable, we found that the *cis*-isomer **7** is energetically preferred by a substantial amount (2.3 kcal/mol).²³ Once formed, **7** would then eliminate the CF_3^- through **7-TS*** to provide the corresponding *cis*-isomer **5A**. The overall barrier of **7-TS*** from **6** is calculated to be 32.4 kcal/mol and is 2.4 kcal/mol lower than **7'-TS*** which gives **5**.

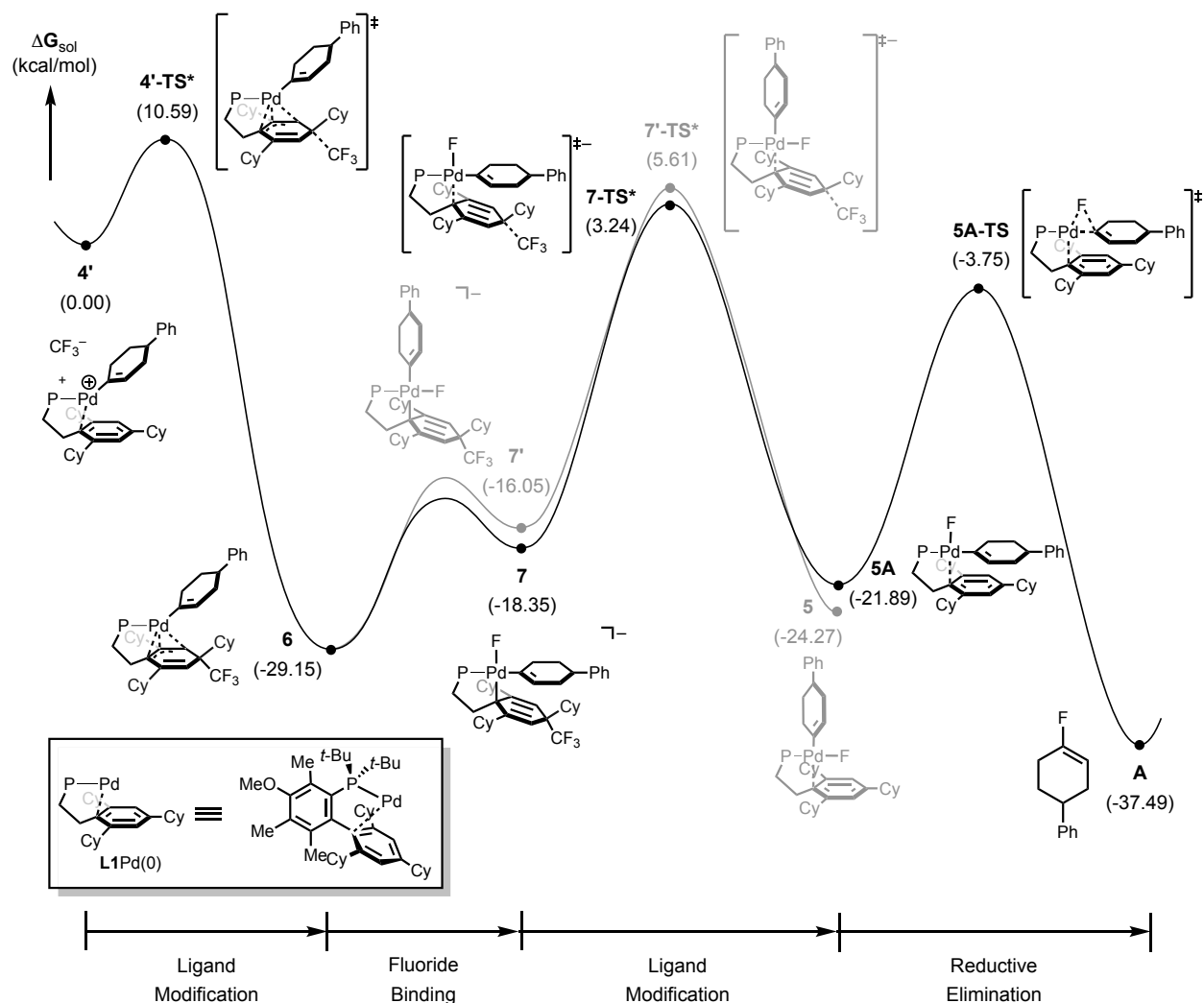
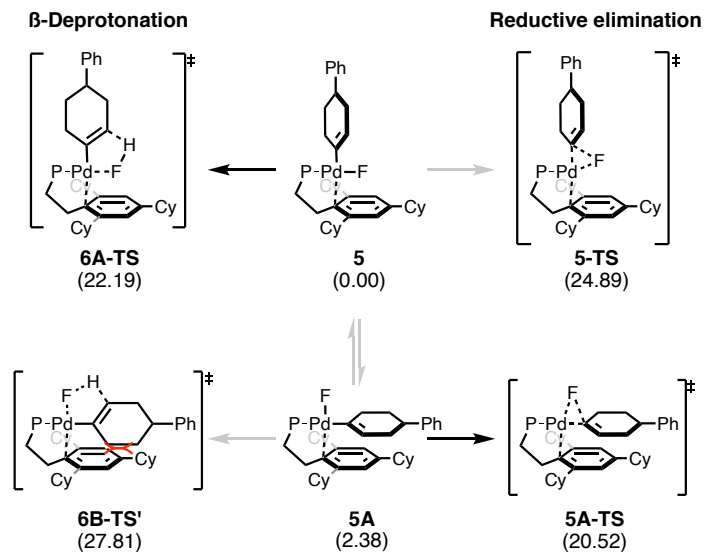


Figure 4. Energy profile of the proposed dearomatization reaction between CF_3^- and **4**. (* represents an estimated barrier. See the Supporting Information for the details)

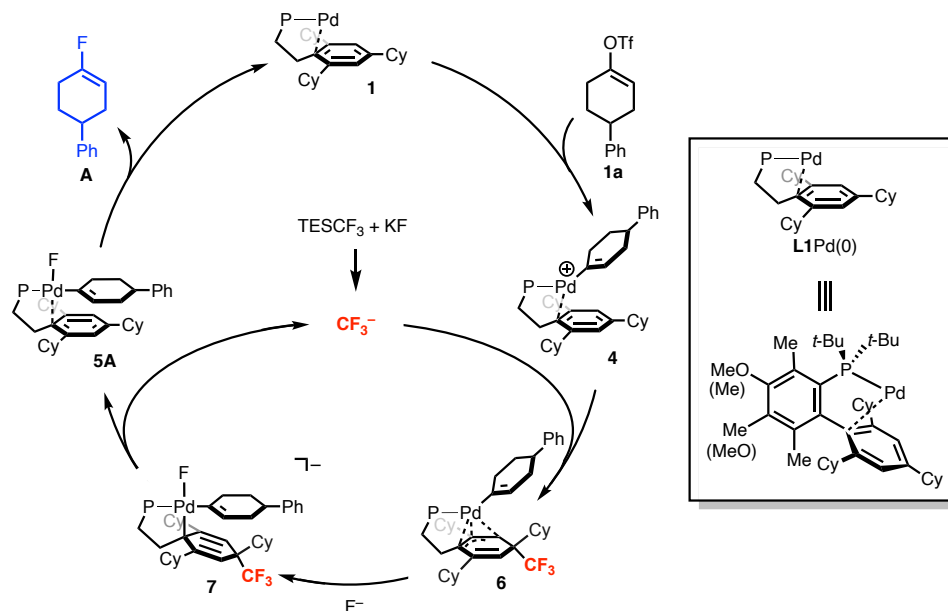
Interestingly, when we investigated the reactivity of **5A** toward either β -deprotonation or reductive elimination, we found that **5A** displays the opposite selectivity to that manifested by **5**. As summarized in Scheme 8, the reductive elimination barrier of **5A** is calculated to be 7.3 kcal/mol lower than that of β -deprotonation pathway, while **5** prefers β -deprotonation. This suggested that **5A** should undergo facile and regioselective reductive elimination to provide the fluorinated product **A**, and no **L1Pd(II)**-cyclohexyne intermediates should be generated (Figure 4). Of importance, the barrier to isomerization between **5** and **5A** was calculated to be ~23.6 kcal/mol, which is higher than either **6A-TS** or **5A-TS**, suggesting that isomerization is unlikely under the reaction conditions that were employed (see Figure 2S in the Supporting Information for more details).

Scheme 8. Reaction Preferences of **5** and **5A**.



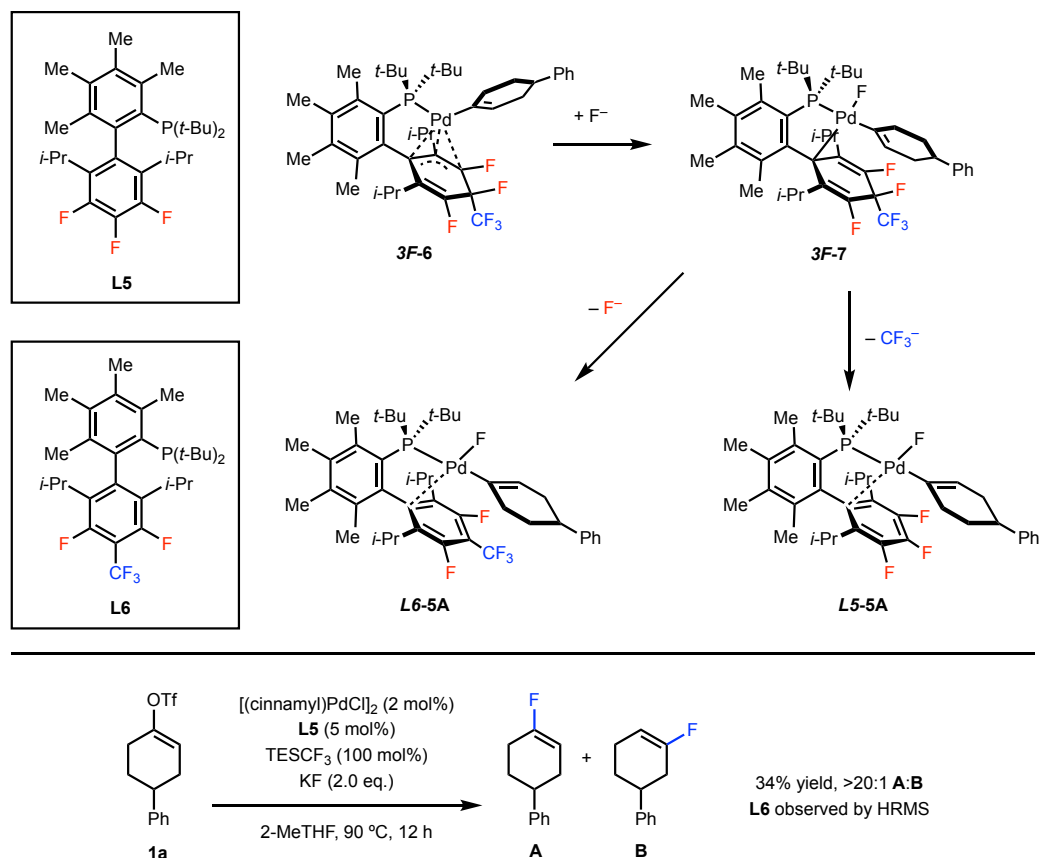
Based on these results, a proposed mechanism for the fluorination of vinyl triflates with TESCF_3 as an additive is illustrated in Scheme 9. During the induction period, TESCF_3 releases CF_3^- . Most of them would be expected to decompose unproductively to form CHF_3 or CF_2CF_2 . Some, however, can react with **4**, which was generated after oxidative addition of **1** with the starting material **1a**, to provide the dearomatized intermediate **6**. The fluoride anion would then react with **6** to form intermediate **7**, which subsequently ejects CF_3^- to generate the *cis*-**L1Pd(vinyl)F 5A**. **5A** would undergo reductive elimination to provide the vinyl fluoride **A** with the desired regioselectivity. Essentially, in the fluorination process with TESCF_3 as an additive, the CF_3^- released actually functions to facilitate the formation of **5A**, which is responsible for the improved regioselectivity of the reaction.

Scheme 9. Proposed Fluorination Mechanism in the Presence of TESCF₃.



In order to obtain experimental evidence for the formation of dearomatized intermediate **6**, we designed a fluoro-substituted ligand **L5**, which could be employed as a probe to determine whether the bottom ring of the ligand ever undergoes nucleophilic attack by CF_3^- (Scheme 10). We hypothesized that in the reaction using **L5** as the ligand and TESCF_3 as an additive, in a manner analogous to the formation of intermediate **6** when **L1** was used, the corresponding intermediate **3F-6** would be generated. In the presence of fluoride, **3F-6** could be converted to **3F-7**, which would undergo rearomatization by losing a CF_3^- to generate **L5-5A**. Alternatively, **3F-7** could also rearomatize by losing a F^- to form **L6-5A**. If the latter pathway is followed, a new ligand **L6**, in which one fluorine was substituted by a trifluoromethyl group, would be generated. When **L5** was used as the ligand in the fluorination reaction using TESCF_3 as the additive, the fluorinated product was formed in 34% yield with >20:1 regioselectivity. ^{31}P NMR analysis of the crude reaction mixture showed that most of the **L5** remained unchanged, and the formation of **L6** could not be verified. However, when we analyzed the crude reaction mixture by HRMS, we unambiguously identified a new peak corresponding to **L6** ($[\text{L6}+\text{H}^+]=543.3174$, found 543.3187, see the Supporting Information for more details). This peak was not seen in control experiments in which either the Pd source or the triflate starting material were omitted, which is consistent with **L6** being formed through the pathway proposed in Scheme 10. Participating by the Pd center may cause **3F-7** to preferentially undergo rearomatization by losing a CF_3^- from the anti face of the aromatic system rather than a F^- group from the syn face. Again, these results are consistent with the proposed *in situ* ligand dearomatization by CF_3^- under the fluorination conditions.

Scheme 10. Generation of Pd complexes Supported by ligand with a dearomatized bottom ring.



Conclusion

In summary, we have investigated the mechanism of the Pd-catalyzed fluorination of cyclic vinyl triflates in the absence or presence of TESCF₃ additives. A combined experimental and computational study suggested that when no TESCF₃ was added, a Curtin–Hammett situation is operative during the fluorination process, which was responsible for the observed low yield and regioselectivity. In the presence of TESCF₃, an alternative pathway involving an unusual dearomatization of the ligand by nucleophilic attack from a CF₃[−] was proposed on the basis of literature precedents and our DFT calculations. Although the stoichiometric preparation and isolation of the dearomatized intermediate was unsuccessful, our results are fully consistent with the hypothesized mechanism.

The significant influence of the *cis/trans*-geometry of Pd(II) fluoride intermediates on the reaction outcome is the key to understanding this fluorination process and the additive effect. The *trans*-isomer (**5**) preferentially undergoes β-deprotonation, which ultimately produces mixtures of product isomers. In contrast, the *cis*-isomer (**5A**) undergoes facile reductive elimination rather than

β -deprotonation to provide the fluorinated product without isomerization. The presence of CF_3^- in the reaction is believed to disfavor the formation of the *trans*-isomer (**5**) through temporary dearomatization of the bottom aryl ring of the ligand. Finally, the unusual transmetalation mechanism disclosed in this study involving an *in situ* ligand modification pathway might be relevant in other cross-coupling processes employing bulky biarylphosphine-derived Pd catalysis.

Associated Content

Supporting Information

The Supporting Information is available free of charge on the ACS Publications website.

Experimental details and computational data (PDF)

Spectroscopic Data (PDF)

Author Information

Corresponding Author

*mbaik2805@kaist.ac.kr

*sbuchwal@mit.edu

Author Contributions

Y. Ye and S.-T. Kim contributed equally.

Notes

The authors declare no competing financial interests.

Acknowledgements

We are grateful to the National Institutes of Health (R35-GM122483), and the Institute for Basic Science (IBS-R010-A1) in Korea. The content is solely the responsibility of the authors and does not necessarily represent the official views of the National Institute of Health. We thank Drs. Richard Liu, Scott McCann, Christine Nguyen, Alex Schuppe, Yang Yang for their advice on the preparation of this manuscript. We acknowledge Charlene Tsay (MIT) for X-ray crystallographic analysis.

References

- (1) O'Hagan, D. Understanding Organofluorine Chemistry. An Introduction to the C–F Bond. *Chem. Soc. Rev.* **2008**, *37*, 308–319.
- (2) (a) Wang, J.; Sánchez-Roselló, M.; Aceña, J. L.; delPozo, C.; Sorochinsky, A. E.; Fustero, S.; Soloshonok, V. A.; Liu, H. Fluorine in Pharmaceutical Industry: Fluorine-Containing Drugs Introduced to the Market in the Last Decade (2001–2011). *Chem. Rev.* **2014**, *114*, 2432–2506. (b) Zhou, Y.; Wang, J.; Gu, Z.; Wang, S.; Zhu, W.; Aceña, J. L.; Soloshonok, V. A.; Izawa, K.; Liu, H. Next Generation of Fluorine-Containing Pharmaceuticals, Compound Currently in Phase II–III Clinical Trials of Major Pharmaceutical Companies: New Structural Trends and Therapeutic Areas. *Chem. Rev.* **2016**, *116*, 422–518. (c) Yamazaki, T.; Taguchi, T.; Ojima, I. Unique Properties of Fluorine and their Relevance to Medicinal Chemistry and Chemical Biology. In *Fluorine in Medicinal Chemistry and Chemical Biology*; John Wiley & Sons: Chichester, U.K., 2009.
- (3) Jeschke, P. The Unique Role of Fluorine in the Design of Active Ingredients for Modern Crop Protection. *ChemBioChem* **2004**, *5*, 570–589.
- (4) (a) Gillis, E. P.; Eastman, K. J.; Hill, M. D.; Donnelly, D. J.; Meanwell, N. A. Applications of Fluorine in Medicinal Chemistry. *J. Med. Chem.* **2015**, *58*, 8315–8359. (b) Hagmann, W. K. The Many Roles for Fluorine in Medicinal Chemistry. *J. Med. Chem.* **2008**, *51*, 4359–4369.
- (5) Balz–Schiemann reaction: Balz, G.; Schiemann, G. Über aromatische Fluorverbindungen, I.: Ein neues Verfahren zu ihrer Darstellung. *Ber. Dtsch. Chem. Ges. B* **1927**, *60*, 1186–1190.; Halex process: Finger, G. C.; Kruse, C. W. Aromatic Fluorine Compounds. VII. Replacement of Aromatic –Cl and –NO₂ Groups by –F^{1,2}. *J. Am. Chem. Soc.* **1956**, *78*, 6034–6037.
- (6) (a) Wang, X.; Mei, T.-S.; Yu, J.-Q. Versatile Pd(OTf)₂·2H₂O-Catalyzed *ortho*-Fluorination Using NMP as a Promoter. *J. Am. Chem. Soc.* **2009**, *131*, 7520–7521. (b) Mazzotti, A. R.; Campbell, M. G.; Tang, P.; Murphy, J. M.; Ritter, T. Palladium(III)-Catalyzed Fluorination of Arylboronic Acid Derivatives. *J. Am. Chem. Soc.* **2013**, *135*, 14012–14015. (c) Hull, K. L.; Anani, W. Q.; Sanford, M. S. Palladium-Catalyzed Fluorination of Carbon–Hydrogen Bonds. *J. Am. Chem. Soc.* **2006**, *128*, 7134–7135. (d) Chan, K. S. L.; Wasa, M.; Wang, X.; Yu, J.-Q. Palladium(II)-Catalyzed Selective Monofluorination of Benzoic Acids Using a Practical Auxiliary: A Weak-Coordination Approach. *Angew. Chem., Int. Ed.* **2011**, *50*, 9081–9084. (e) Perez-Temprano, M. H.; Racowski, J. M.; Kampf, J. W.; Sanford, M. S. Competition Between sp³-C–N vs sp³-C–F Reductive Elimination from Pd^{IV} Complexes. *J. Am. Chem. Soc.* **2014**, *136*, 4097–4100. (f) Ball, N. D.; Sanford, M. S. Synthesis and Reactivity of a Mono-σ-Aryl Palladium(IV) Fluoride Complex. *J. Am. Chem. Soc.* **2009**, *131*, 3796–3797. (g) Furuya, T.; Benitez, D.;

Tkatchouk, E.; Strom, A. E.; Tang, P.; Goddard, W. A.; Ritter, T. Mechanism of C–F Reductive Elimination from Palladium(IV) Fluorides. *J. Am. Chem. Soc.* **2010**, *132*, 3793–3807. (h) Ding, Q.; Ye, C.; Pu, S.; Cao, B. Pd(PPh₃)₄-Catalyzed Direct *ortho*-Fluorination of 2-Arylbenzothiazoles with an Electrophilic Fluoride *N*-Fluorobenzenesulfonimide (NFSI). *Tetrahedron* **2014**, *70*, 409–416. (i) Lou, S.-J.; Xu, D.-Q.; Xia, A.- B.; Wang, Y.-F.; Liu, Y.-K.; Du, X.-H.; Xu, Z.-Y. Pd(OAc)₂-Catalyzed Regioselective Aromatic C–H Bond Fluorination. *Chem. Commun.* **2013**, *49*, 6218–6220.

(7) (a) Grushin, V. V. The Organometallic Fluorine Chemistry of Palladium and Rhodium: Studies toward Aromatic Fluorination. *Acc. Chem. Res.* **2010**, *43*, 160–171. (b) Grushin, V. V.; Marshall, W. J. Ar–F Reductive Elimination from Palladium(II) Revisited. *Organometallics* **2007**, *26*, 4997–5002. (c) Grushin, V. V. Palladium Fluoride Complexes: One More Step toward Metal Mediated C–F Bond Formation. *Chem. -Eur. J.* **2002**, *8*, 1006–1014. (d) Yandulov, D. V.; Tran, N. T. Aryl-Fluoride Reductive Elimination from Pd(II): Feasibility Assessment from Theory and Experiment. *J. Am. Chem. Soc.* **2007**, *129*, 1342–1358.

(8) (a) Watson, D. A.; Su, M.; Teverovskiy, G.; Zhang, Y.; Garcia-Fortanet, J.; Kinzel, T.; Buchwald, S. L. Formation of ArF from LPdAr(F): Catalytic Conversion of Aryl Triflates to Aryl Fluorides. *Science*, **2009**, *325*, 1661–1664. (b) Sather, A. C.; Buchwald, S. L. The Evolution of Pd⁰/Pd^{II}-Catalyzed Aromatic Fluorination. *Acc. Chem. Res.* **2016**, *49*, 2146–2157. (c) Lee, H. G.; Milner, P. J.; Buchwald, S. L. An Improved Catalyst System for the Pd-Catalyzed Fluorination of (Hetero)Aryl Triflates. *Org. Lett.* **2013**, *15*, 5602–5605. (d) Lee, H. G.; Milner, P. J.; Buchwald, S. L. Pd-Catalyzed Nucleophilic Fluorination of Aryl Bromides. *J. Am. Chem. Soc.* **2014**, *136*, 3792–3795. (e) Sather, A. C.; Lee, H. G.; De La Rosa, V. Y.; Yang, Y.; Müller, P.; Buchwald, S. L. A Fluorinated Ligand Enables Room-Temperature and Regioselective Pd-Catalyzed Fluorination of Aryl Triflates and Bromides. *J. Am. Chem. Soc.* **2015**, *137*, 13433–13438. (f) Milner, P. J.; Yang, Y.; Buchwald, S. L. In-Depth Assessment of the Palladium-Catalyzed Fluorination of Five-Membered Heteroaryl Bromides. *Organometallics* **2015**, *34*, 4775–4780.

(9) (a) Maimone, T. J.; Milner, P. J.; Kinzel, T.; Zhang, Y.; Takase, M. K.; Buchwald, S. L. Evidence for in Situ Catalyst Modification during the Pd-Catalyzed Conversion of Aryl Triflates to Aryl Fluorides. *J. Am. Chem. Soc.* **2011**, *133*, 18106–18109. (b) Milner, P. J.; Maimone, T. J.; Su, M.; Chen, J.; Müller, P.; Buchwald, S. L. Investigating the Dearomative Rearrangement of Biaryl Phosphine-Ligated Pd(II) Complexes. *J. Am. Chem. Soc.* **2012**, *134*, 19922–19934. (c) Milner, P. J.; Kinzel, T.; Zhang, Y.; Buchwald, S. L. Studying Regioisomer Formation in the Pd-

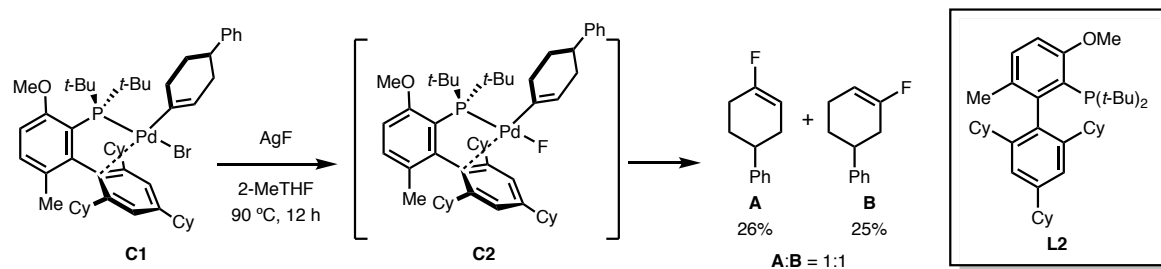
Catalyzed Fluorination of Aryl Triflates by Deuterium Labeling. *J. Am. Chem. Soc.* **2014**, *136*, 15757–15766.

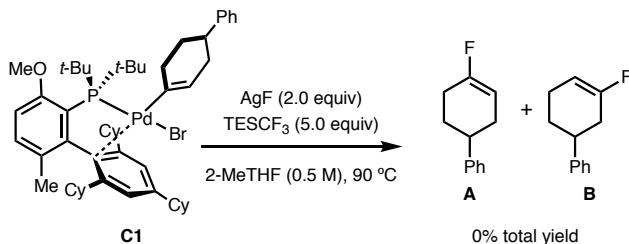
(10) For reviews, see: (a) Purser, S.; Moore, P. R.; Swallow, S.; Gouverneur, V. Fluorine in Medicinal Chemistry. *Chem. Soc. Rev.* **2008**, *37*, 320–330. (b) Neumann, C. N.; Ritter, T. Late-Stage Fluorination: Fancy Novelty or Useful Tool. *Angew. Chem. Int. Ed.* **2015**, *54*, 3216–3221. (c) Kirk, K. L. Fluorination in Medicinal Chemistry: Methods, Strategies, and Recent Developments. *Org. Process Res. Dev.* **2008**, *12*, 305–321. (d) Müller, K.; Faeh, C.; Diederich, F. Fluorine in Pharmaceuticals: Looking Beyond Intuition. *Science* **2007**, *317*, 1881–1886. [SEP]

(11) (a) Welch, J.; Lin, J. Fluoroolefin Containing Dipeptide Isosteres as Inhibitors of Dipeptidyl Peptidase IV(CD26). *Tetrahedron* **1996**, *52*, 291–304. (b) Narumi, T.; Hayashi, R.; Tomita, K.; Kobayashi, K.; Tanahara, N.; Ohno, H.; Naito, T.; Kodama, E.; Matsuoka, M.; Oishi, S.; Fujii, N. Synthesis and Biological Evaluation of Selective CXCR4 Antagonists Containing Alkene Dipeptide Isosteres. *Org. Biomol. Chem.* **2010**, *8*, 616–621. (c) Lamy, C.; Hofmann, J.; Parrot-Lopez, H.; Goekjian, P. Synthesis of a Fluoroalkene Peptidomimetic Precursor of N-Acetyl-1-Glutamyl-1-Alanine. *Tetrahedron Lett.* **2007**, *48*, 6177–6180. (d) Niida, A.; Tomita, K.; Mizumono, M.; Tanigaki, H.; Terada, T.; Oishi, S.; Otaka, A.; Inui, K.-I.; Fuji, N. Unequivocal Synthesis of (*Z*)-Alkene and (*E*)-Fluoroalkene Dipeptide Isosteres to Probe Structural Requirements of the Peptide Transporter PEPT1. *Org. Lett.* **2006**, *8*, 613–616. (e) Niida, A.; Mizumoto, M.; Narumi, T.; Inokuchi, E.; Oishi, S.; Ohno, H.; Otaka, A.; Kitaura, K.; Fujii, N. Synthesis of (*Z*)-Alkene and (*E*)-Fluoroalkene-Containing Diketopiperazine Mimetics Utilizing Organocopper-Mediated Reduction-Alkylation and Diastereoselectivity Examination Using DFT Calculations. *J. Org. Chem.* **2006**, *71*, 4118–4129.

(12) Ye, Y.; Takada, T.; Buchwald, S. L. Palladium-Catalyzed Fluorination of Cyclic Vinyl Triflates: Effect of TESCF₃ as an Additive. *Angew. Chem., Int. Ed.* **2016**, *55*, 15559–15563.

(13) When **L2**Pd(vinyl)Br (**C1**) was treated with AgF, fluorinated products were formed (see Scheme 4). However, no products were observed in the presence of TESCF₃.





- (14) (a) Zhao, Y.; Truhlar, D. G. The M06 Suite of Density Functionals for Main Group Thermochemistry, Thermochemical Kinetics, Noncovalent Interactions, Excited States, and Transition Elements: Two New Functionals and Systematic Testing of Four M06-Class Functionals and 12 Other Functionals. *Theor. Chem. Acc.* **2008**, 120, 215–241. (b) Ditchfield, R.; Hehre, W. J.; Pople, J. A. Self-Consistent Molecular-Orbital Methods. IX. An Extended Gaussian-Type Basis for Molecular-Orbital Studies of Organic Molecules. *J. Chem. Phys.* **1971**, 54, 724–728. (c) Hay, P. J.; Wadt, W. R. *Ab initio* Effective Core Potentials for Molecular Calculations. Potentials for the Transition Metal Atoms Sc to Hg. *J. Chem. Phys.* **1985**, 82, 270–283. (d) Wadt, W. R.; Hay, P. J. *Ab initio* Effective Core Potentials for Molecular Calculations. Potentials for Main Group Elements Na to Bi. *J. Chem. Phys.* **1985**, 82, 284–298. (e) Hay, P. J.; Wadt, W. R. *Ab initio* Effective Core Potentials for Molecular Calculations. Potentials for K to Au Including the Outermost Core. *J. Chem. Phys.* **1985**, 82, 299–310. (f) Dunning, T. H., Jr. Gaussian Basis Sets for Use in Correlated Molecular Calculations. I. The Atoms Boron Through Neon and Hydrogen. *J. Chem. Phys.* **1989**, 90, 1007–1023.
- (15) Liu, X.; Xu, C.; Wang, M.; Liu, Q. Trifluoromethyltrimethylsilane: Nucleophilic Trifluoromethylation and Beyond. *Chem. Rev.* **2015**, 115, 683–730.
- (16) Prakash, G. K. S.; Wang, F.; Zhang, Z.; Haiges, R.; Rahm, M.; Christe, K. O.; Mathew, T.; Olah, G. A. Long-Lived Trifluoromethanide Anion: A Key Intermediate in Nucleophilic Trifluoromethylations. *Angew. Chem. Int. Ed.* **2014**, 53, 11575–11578.
- (17) Lishchynskiy, A.; Miloserdov, F. M.; Martin, E.; Benet-Buchholz, J.; Escudero-Adán, E. C.; Konovalov, A. I.; Grushin, V. V. The Trifluoromethyl Anion. *Angew. Chem. Int. Ed.* **2015**, 54, 15289–15293.
- (18) Cho, E. J.; Buchwald, S. L. The Palladium-Catalyzed Trifluoromethylation of Vinyl Sulfonates. *Org. Lett.* **2011**, 13, 6552–6555.
- (19) Ueda, S.; Ali, S.; Fors, B. P.; Buchwald, S. L. Me₃(OMe)*t*BuXPhos: A Surrogate Ligand for Me₄*t*BuXPhos in Palladium-Catalyzed C–N and C–O Bond-Forming Reactions. *J. Org. Chem.* **2012**, 77, 2543–2547.

- (20) (a) Our attempts to prepare **L2**Pd(vinyl)CF₃ from either **L2**Pd(vinyl)Br or **L2**Pd(vinyl)OTf all provided <5% of **L2**Pd(vinyl)CF₃, as observed by ¹⁹F NMR analysis of the crude reaction mixture. (b) Pu, M.; Sanhueza, I. A.; Senol, E.; Schoenebeck, F. Divergent Reactivity of Stannane and Silane in the Trifluoromethylation of Pd^{II}: Cyclic Transition State versus Difluorocarbene Release. *Angew. Chem. Int. Ed.* **2018**, *57*, 15081–15085. (c) Cho, E. J.; Senecal, T. D.; Kinzel, T.; Zhang, Y.; Watson, D. A.; Buchwald, S. L. The Palladium-Catalyzed Trifluoromethylation of Aryl Chlorides. *Science* **2010**, *328*, 1679–1681.
- (21) (a) Allgeier, A. M.; Shaw, B. J.; Hwang, T.-L.; Milne, J. E.; Tedrow, J. S.; Wilde, C. N. Characterization of Two Stable Degradants of Palladium *t*BuXPhos Catalyst and a Unique Dearomatization Reaction. *Organometallics* **2012**, *31*, 519–522. (b) Lee, H. G.; Milner, P. J.; Colvin, M. T.; Andreas, L.; Buchwald, S. L. Structure and Reactivity of [(LPd)_n(1,5-cyclooctadiene)] (n = 1–2) Complexes Bearing Biaryl Phosphine Ligands. *Inorganic Chimica Acta*, **2014**, *422*, 188–192. (c) Lee, H. G.; Milner, P. J.; Buchwald, S. L. An Improved Catalyst System for the Pd-Catalyzed Fluorination of (Hetero)Aryl Triflates. *Org. Lett.* **2013**, *15*, 5602–5605.
- (22) Based on calculations, attacking by CF₃[−] has a lower energy barrier than by CF₂ carbene (see the Supporting Information for details).
- (23) The trifluoromethylative dearomatization of the bottom ring of **L1** places a negative charge on the aryl component and turns the weakly coordinating, neutral, π-basic arene ligand into a stronger, anionic donor ligand. Accordingly, the energy preference for the *trans*-isomer (*trans*-effect) becomes insignificant and the computed electronic energies of the two isomers become equal. The preference for the *cis*-isomer is therefore governed by solvation energy (see the Supporting Information for details).